NUMERICAL ANALYSIS OF A VERTICAL ASCENDANT TWO-PHASE FLOW IN A CYCLONIC CHAMBER UNDER THE ACTION OF CENTRIFUGAL AND GRAVITATIONAL FIELDS

Henrique Krainer Eidt, hkeidt@gmail.com[1]
Carolina Cimarelli Rodrigues, carolcimarelli@gmail.com[2]
Paulo Henrique Dias dos Santos, psantos@utfpr.edu.br[3]
Rigoberto Eleazar Melgarejo Morales, rmorales@utfpr.edu.br[4]
1, 2, 3, 4 Universidade Tecnológica Federal do Paraná, Avenida Sete de Setembro 3165, Rebouças, CEP: 80230-901, Curitiba, Paraná.

Abstract. *In the petroleum industry equipment capable of separating the liquid and gas phases of two-phase flow are necessary, in order to use centrifugal pumps. The existing pieces of equipment are generally oversized, which makes them harder to be installed on the seabed. An alternative would be the use of smaller centrifugal separators. Thus, in this work, a numerical analysis of a distribution system is performed prior to the centrifugal separators. This system has a cyclonic chamber. The two-phase flow gets into this chamber tangentially and a vertical ascendant flow liquid film is formed, influenced by the action of the centrifugal and gravitational fields. The performance of separation is analyzed, regarding the mass flow rate in the exits of the distribution system. For the numerical simulations the finite volume method based on finite element (ANSYS-CFX software 15.0) is used, apart from the models two fluids Eulerian-Eulerian inhomogeneous and turbulence SST (Shear Stress Transport). For capturing the liquid-gas interface the compressive advection discretization scheme is used.*

Keywords*: distribution system, numerical analysis, liquid film, vertical ascendant flow, gravitational and centrifugal field.*

1. INTRODUCTION

In the petroleum industry, during the production and transportation of oil, two-phase flow occurs, due to the usual mixture of the crude oil, water and gas. Separating gaseous and liquid phases at the wellhead level has innumerous advantages, such as avoiding or at least reducing typical problems of multiphase flows (intermittent flow, severe slugging, hydrates deposition). Another advantage is the increase in the efficiency of the submersible centrifugal pumps or any artificial lift process used. The equipment that separates the phases is called Separator and the two models most frequently used in offshore installations are: the Vertical Annular and Pumping System (VASPS) and the Gas-Liquid Cylindrical Cyclone (GLCC). The concept of the centrifugal field to divide the phases and to separate the mixture faster than conventional gravitational separators (Ninahuanca, 2013) is the reason why they are used.

Facilities and maintenance of these separators are hampered by the large size of this type of equipment (Morandin, 1999). Therefore, a prior distribution system is proposed in order to decrease the geometry of the separator, while maintaining the flow rate and separation efficiency. To keep these parameters is necessary to implement more separators with reduced dimensions. The flow division occurs through a distributor which is shown schematically in Figure 1, in which the entries are located at the bottom and exits at the top, all placed tangentially to the cyclonic chamber.

An upward flow of liquid film, driven by centrifugal fields, results when the liquid-gas mixture enters the distributor, due to the tangential position of the inlets and the curvature of the cyclonic chamber. This flow has the characteristic in which a thin liquid film flows near the wall under the action of centrifugal and gravitational fields until it is divided in four outlets. Inside the VASPS's expansion chamber there is also the formation of a liquid film, however, the flow is downward.

Some authors carried out studies on the behavior and development of a liquid downward film flow under the effect of centrifugal and gravitational fields. Morandin (1999) accomplished a theoretical, numerical and experimental study within the cyclonic chamber VASPS separator and has determined, using dimensional analysis, that the film flow representative dimensionless numbers are the film Reynolds number, $Re_{\delta f}$, and a squared Froude number, Fr^2_{Qf}, given by:

$$Re_{\delta f} = \frac{Q_L}{2\pi R_0 \nu} \tag{1}$$

$$Fr^2_{Qf} = \frac{Q_L^2}{g R_0^5} \tag{2}$$

where Q_L is the volumetric flow rate [m³/s], R_0 is the expansion chamber radius, g is the gravity acceleration and ν is the kinematic viscosity.

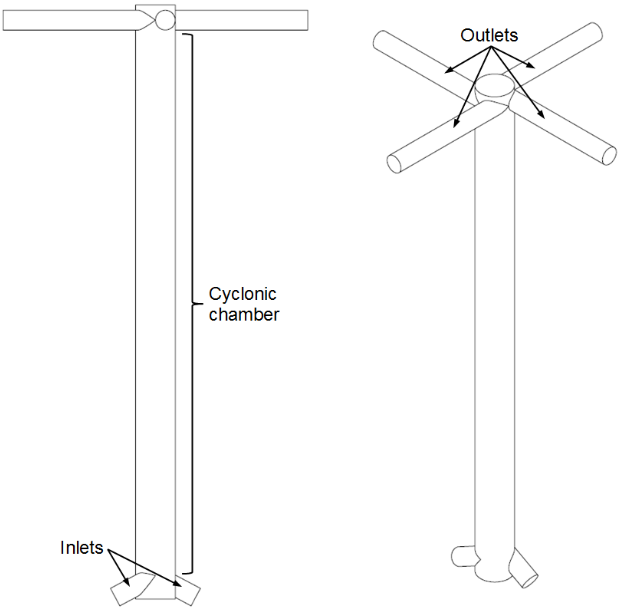

Figure 1. Schematic representation of the distributor.

Morandin (1999) has also demonstrated that the larger the Froude number, the better will be the conditions for the formation of a symmetrical flow throughout the cross section of the expansion chamber. Sant'anna (2010) carried out a numerical study in the interior of the VASPS separator's expansion chamber, validated with experimental data Morandin (1999), and concluded that the behavior of the liquid film flow within this expansion chamber do not depends on the gas phase. Ofuchi (2012) carried out a numerical study of the liquid film behavior in the same expansion chamber and developed a model to determine the lifting height of the liquid level in the chamber, the average film thickness, the residence time fluid into the separator, the inclination angle of the streamlines in the chamber outlet and the separation rate. The correlations were determined based on dimensionless parameters $Re_{\delta f}$ and Fr_{Qf}^2. According to the author, the liquid film thickness increases with the increase of Froude number and the decrease of Reynolds number for both laminar and turbulent flows. Ninahuanca (2015) carried out a numerical and experimental study of characterization of the descending liquid film flow under the effect of centrifugal and gravitational fields in the VASPS separator's expansion chamber, and developed a mathematical model. This model uses the concept of a streamline average for the analysis of the thickness and the velocity of the liquid film. Such parameters varied depending on the dimensionless numbers $Re_{\delta f}$ and Fr_{Qf}^2.

The present study carried out a numerical analysis of the upward liquid film flow behavior under the effect of centrifugal and gravitational fields and of the flow distribution in the outlets. The relevance of this work is due to the need for equitable distribution of liquid and gas flow rates, which is provided by the uniformity and stability of the thickness of the liquid film at the outlet of the distribution system's cyclonic chamber. Besides, according to the author's knowledge there not exist any study regarding to the behavior of vertical ascendant liquid film flow.

2. NUMERICAL MODEL

Once this work is focused on the behavior of the liquid film flow upward, it will not be held an analysis for the gaseous phase flow. This phenomenon can be understood as a liquid and gas field wherein both phases are continuous and separated by a free surface interface. This problem can be solved through the mass and momentum balances for each phase within the domain as well as the resolution of an interface between them. The ANSYS CFX was used for this solution.

2.1 Mathematical modeling

The Eulerian-Eulerian approach is available in ANSYS CFX 15.0 program for simulations of two-phase transient flow. This procedure assumes an inertial frame of reference for each phase, which are regarded as interpenetrating and continuous. The method used in this work is inhomogeneous, meaning that flow fields for each phase are calculated and the interfacial interactions between them are taken into account through source terms.

The Eulerian-Eulerian inhomogeneous approach is achieved using a phase indicator function and an averaging process on the local transport equations. The purpose of this procedure is to transform a two-phase discontinuous mediums in two continuous separate mediums, one for each phase (Yeoh and You, 2009). Neglecting the interfacial mass transfer between different phases and the non-drag forces, the mass conservation equations and the balance of momentum to phase "k" can be written respectively as:

$$\frac{\partial \alpha_k \rho_k}{\partial t} + \nabla \cdot \left(\alpha_k \rho_k \hat{\mathbf{v}}_k \right) = 0 \tag{3}$$

$$\frac{\partial \alpha_k \rho_k \hat{\mathbf{v}}_k}{\partial t} + \nabla \cdot \left(\alpha_k \rho_k \hat{\mathbf{v}}_k \hat{\mathbf{v}}_k \right) = -\nabla \left(\alpha_k p_k \right) + \nabla \cdot \left[\alpha_k \left(\tau_k + \tau_k^T \right) \right] + \alpha_k \rho_k \mathbf{g}_k + \mathbf{F}_D \tag{4}$$

where α_k is the volume fraction of phase k, ρ_k is the density, $\hat{\mathbf{v}}_k$ is the mass-averaged phase velocity, $\mathbf{F}_D$ is the drag force per volume unit between phases, p_k is the pressure, $\mathbf{g}_k$ is the gravity, τ_k is the viscous stress tensor and τ_k^T is the Reynolds stress tensor which results from the Reynolds averaging. The Reynolds tensor is modeled using the eddy viscosity approach and the SST model (Shear Stress Transport) (Wilcox, 1998).

One of the disadvantages of the two-phase Eulerian-Eulerian approach in the context of the free surface flow is that the presence of each phase is smoothed in space, since the phases are considered continuous and interpenetrating. Thus, the interface between the layers tends to be too diffuse in the space, meaning it has nonzero thickness. One way to determine the location of the liquid-gas interface is adopting a compressive discretization scheme to reduce the probability range where the interface is located, which is a numerical technique applied on the advection term of volume fraction equation.

The interaction force at the liquid-gas interface, $\mathbf{F}_D$, is calculated by the drag force model being considered as a free surface, which can be expressed as:

$$\mathbf{F}_D = C_D \rho_{ij} A_{ij} \left(v_j - v_i \right) \left| v_j - v_i \right| \tag{5}$$

where C_D is the drag coefficient, ρ_{ij} is the mixture density, define as $\rho_{ij} = \alpha_i\rho_i + \alpha_j\rho_j$, the subscripts i and j refer to each phase, and A_{ij} is the interfacial area density, define as $A_{ij} = |\nabla\alpha_L|$, where L indicates the liquid phase. In flow with free surface, the drag coefficient for the interaction force at the liquid-gas interface can be set to the value CD = 0.44. This value was regarded as a numerically stable choice as a way of artificially model the phases as continuous and homogeneous (Ansys, 2015).

2.2 Computational Mesh

Figure 2 shows the finite elements distribution in the computational grid of the fluid domain of the analyzed geometry with around 2,500,000 elements. The mesh was built from tetrahedral and hexahedral elements. In order to have a mesh refinement (increasing the density of volume elements), refined prismatic elements extruded were used near the cyclonic chamber wall so that the simulations could provide more details of the free surface interface and conform to the wall law to allow the use of model SST turbulence. This model requires that the distance dimensionless $y+ < 2$, wherein:

$$y^+ = \frac{\Delta n}{\nu} \sqrt{\frac{\tau_\omega}{\rho}} \tag{6}$$

where Δn is the distance between the first and the second integration point from the wall, ν is the kinematic viscosity, ρ is the fluid density and τ_ω is the wall shear stress (Ansys, 2015).

The distance between this liquid-gas interface and the cyclonic chamber wall is called the liquid film thickness, and will be analyzed in this study.

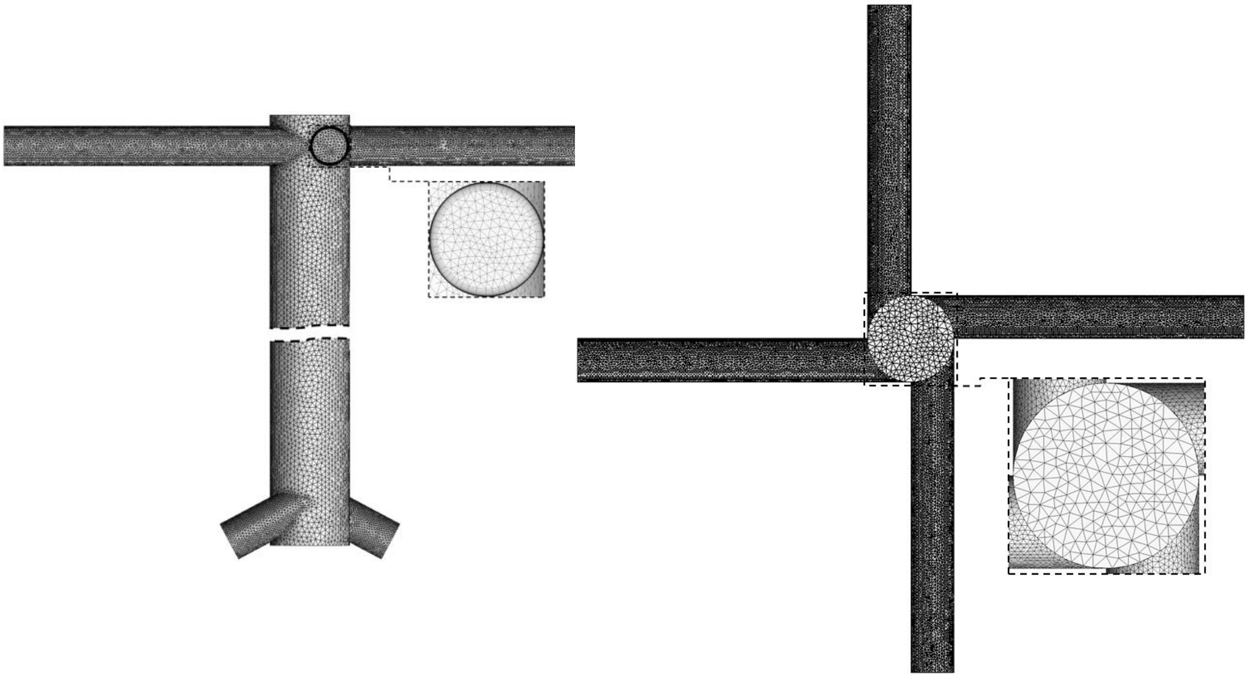

Figure 2. Computational mesh.

3. RESULTS

This section analyzes the upward liquid film flow under the effect of centrifugal and gravitational fields, and the flow division on the distributor outlets. At the cyclonic chamber entrances the flow is intermittent, pulsing alternately liquid and gas, in order to represent the slug pattern. The operating conditions (liquid and gas velocities) were obtained from the model developed by Barnea et al. (1982) for a vertical upward flow with liquid and gas of 997 kg / m³ and 1.185 kg / m³, respectively.

The apparent liquid and gas velocities have been selected considering one of the most critical cases for slug flow of the Barnea et al. model (1982). The dimensionless Reynolds and Froude numbers, corresponding to operating conditions of the study, are 17,000 and 84, respectively.

Therefore, in the present work was carried out a numerical analysis of the liquid film behavior in the cyclonic chamber, and the liquid and gas phases division in the distributor outlets. The total simulation time was four seconds, with a timestep of 0.0025 seconds saved every 16 timestep.

The Figure 3 depicts schematically a slug flow and how the intermittence of this pattern is treated in the present work. From the input condition, the liquid and gas velocities were determined, as well as the intermittence time for each phase.

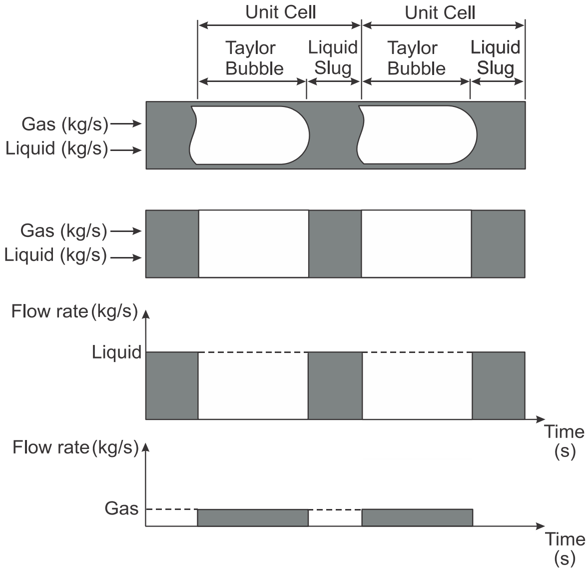

Figure 3. Representative scheme of the pulsation between liquid and gas flows.

3.1 Analysis of the flow rates distribution at the outlets

Based on numerical simulation it was possible to analyze the liquid-gas flow distribution in the distributor outlets. The percentage comparison concerning the temporal average of the volume fraction at the outlets and horizontal tubes is shown in Table 1, with the aim of analyze the volumetric quantity of the phases. To achieve the results, the calculation of the average in time of the volume fraction on the surface of the horizontal tubes and outlets was carried out, and compared with the average of the four horizontal pipes and four outlets respectively.

Table 1. Comparison of the volume fraction at the distributor outlets and horizontal pipes.

	Volume fraction in outlets	Volume fraction in horizontal tubes
Outlet 1	6.45%	1.03%
Outlet 2	8.51%	0.67%
Outlet 3	1.44%	1.28%
Outlet 4	7.57%	0.41%

Table 1 shows the proximity of the volume fractions divisions at the four outlets, with a maximum difference of 9% approximately and when compared to the volume fraction in the entire horizontal pipeline the maximum difference between them decreases even more, reaching almost 1 %. This reduction occurs because the pipeline area analyzed is significantly larger than the area of the outlet, reducing the errors due to the number of saved timesteps. Therefore, it can be said that this type of distributor performs an approximately equitable liquid and gas flow rates distribution.

Figure 4 shows the volume fraction average distribution in four horizontal pipelines. From this figure and Table 1, it’s possible to note a similarity in the horizontal pipes flow, which can indicate an equitable distribution of the flow. Furthermore, as the flow becomes horizontal, a pre phase separation near the outlets occurs, developing a stratified flow, which can facilitate the liquid-gas separation in the separators.

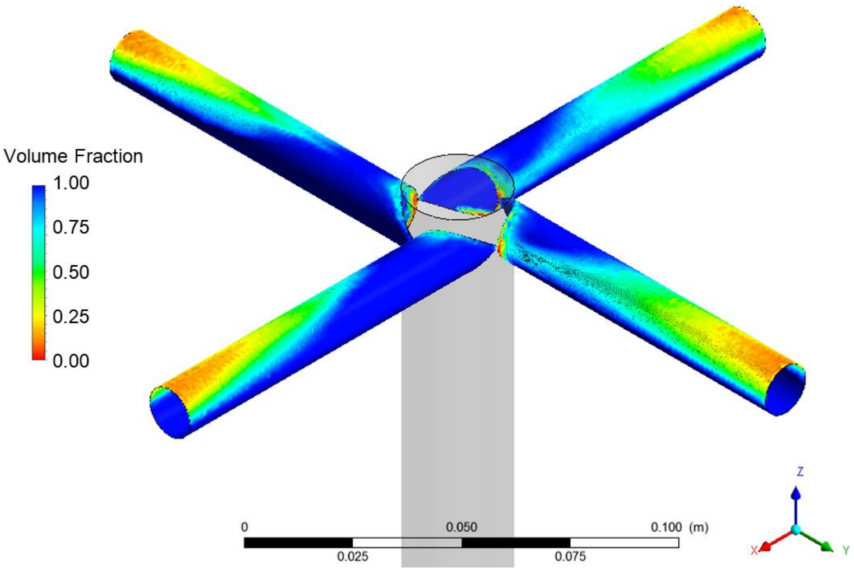

Figure 4. Average volume fractions distribution at the four pipes outlets.

Table 2 compares the difference of the liquid and gas mass flow rates with the four outlets time average. As the differences in liquid and gas volumetric quantities at the outlets are low, as shown in Table 1, the mass flow rates also have the same behavior and consequently also the phases velocities.

Table 2. Liquid and gas flow rate comparison.

	Liquid mass flow	Gas mass flow
Outlet 1	1.55%	2.41%
Outlet 2	6.05%	8.20%
Outlet 3	0.32%	1.14%
Outlet 4	4.82%	6.92%

3.2 Analysis of the liquid film behavior in the cyclonic chamber

After performing the analysis of the flow division at the distributor outputs the study of the liquid film flow behavior on the cyclonic chamber is carried out. Eq. 7 computes the time average thickness of the liquid film in the cyclonic chamber. Fig. 5 shows the value of time average thickness by the length of the cyclonic chamber and it can be seen that this average has an increasing trend until it reaches the of height of 275mm. Then it is replaced by a behavior with low variation. At the height of 375mm, the thickness has large fluctuations due to the proximity of the distributor outlets.

$$\bar{\delta} = \frac{1}{\Delta t}\int_{\Delta t}\left[R_c - \frac{1}{2}\sqrt{4R_c^2 - \frac{4A_z}{\pi}}\right]dt \qquad A_z = \int_{A_z} dA \tag{7}$$

where Δt is the total simulation time, R_c is the radius of the cyclonic chamber and A_z is the cross-sectional area of the fluid at each length of the cyclonic chamber shown in Fig. 6.

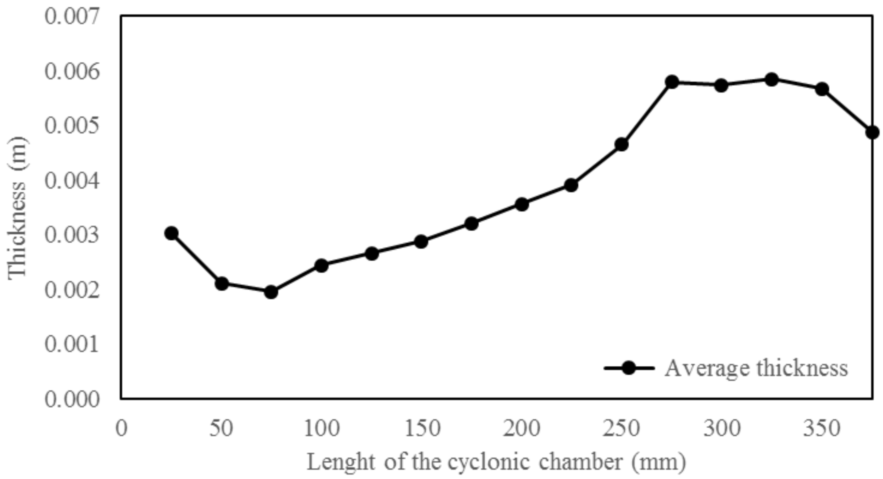

Figure 5. The average liquid film thickness in the cyclonic chamber.

Thickness variation shown in Figure 5 can be best seen in Figure 7 in which the profile of the time average of the liquid film thickness in the cyclonic chamber is presented. It may be noted that the thickness of the liquid film at the bottom of the cyclonic chamber is thin and the lenght the liquid film gets the thicker it becomes. It is believed that this occurs because, as the flow distances itself from the cyclonic chamber's inlets, the influence of the centrifugal field decreases due to shear tensions. Therefore, the influence of the gravitational field stands out. Fig. 6 also shows the planes where the average thickness and the average velocities related to the liquid film were calculated.

Figure 7 shows the graphs of the module of average velocity vector and the average axial velocity along the length of the cyclonic chamber calculated by Eq. 8 and Eq. 9 in the same planes shown in Fig. 6. A gradual decrease in the values of both velocities can be observed. This happens because the gravitational field and the shear stress acts in an opposite direction of the flow. A comparison between Figure 5 and Figure 7-(b) can show that the increase in average thickness is a consequence of the reduced axial velocity, the sections 50mm to 275mm, the thickness increases as the axial velocity decreases, and from 275mm to 350mm that the thickness and the axial velocity do not vary significantly.

$$\bar{V} = \frac{1}{A_z \Delta t}\int_{\Delta t}\int_{A_z}\left(\vec{V}\cdot\vec{n}\right)dA_z dt \tag{8}$$

$$\bar{V}_z = \frac{1}{A_z \Delta t}\int_{\Delta t}\int_{A_z} V_z dA_z dt \tag{9}$$

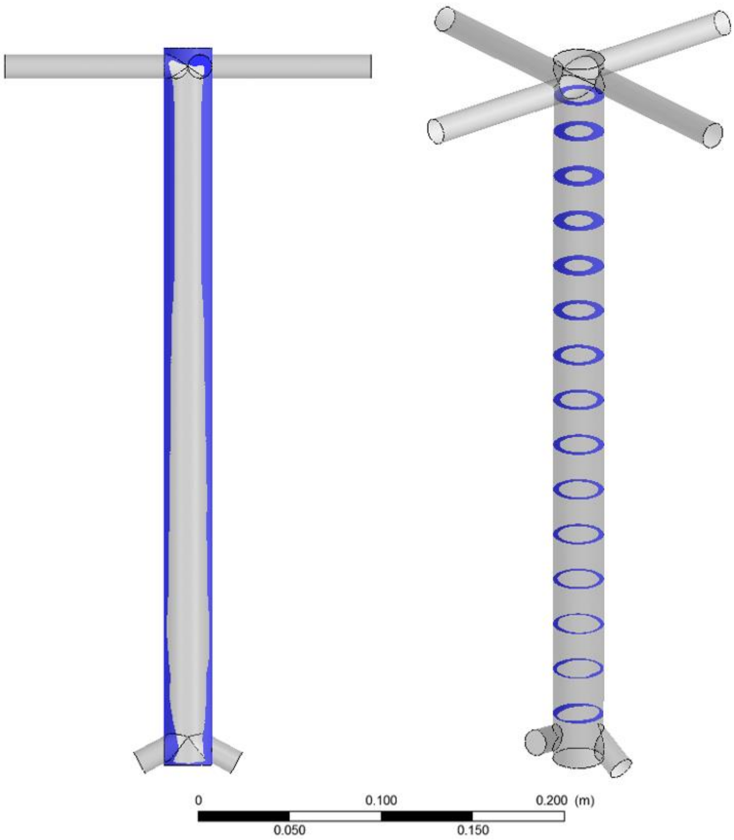

Figure 6. Average thickness in the cyclonic chamber.

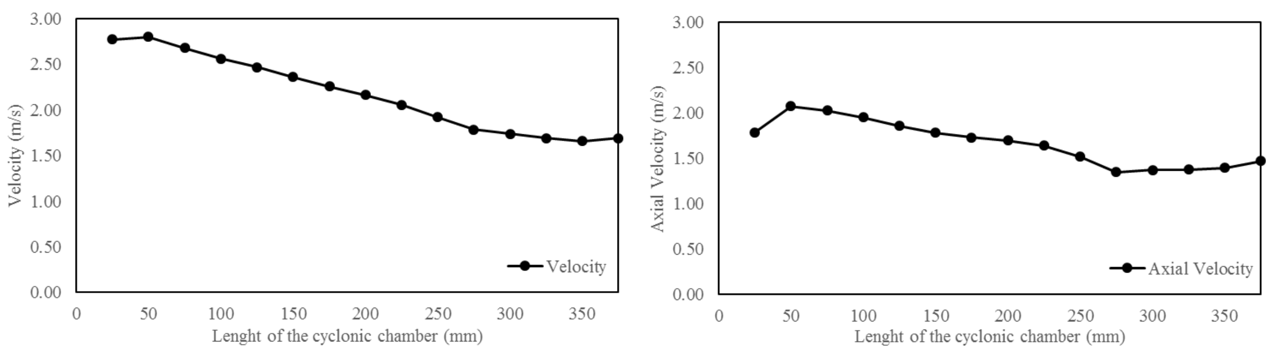

(a) (b)

Figure 7. (a) Module vector average velocity along the cyclonic chamber. (b) Average axial velocity along the cyclonic chamber.

The drag force and the gravitational field acting against the flow cause the reduction of the vector velocity. However, it is noted that the shear stress acts more strongly in the liquid film than in the gravitational field, since the tangential velocity undergoes further reduction than the axial and radial velocities. Thus, the angle of the current lines, calculated by Eq. 10, increases with the length of the cyclonic chamber, as it can be seen in Figure 8. If Figure 7-(b) and Figure 8 are analyzed together, one can notice that for heights greater than 275mm, the axial velocity is not decreased, though, the average angle of the current lines continues to rise.

$$\theta = \arcsin\left(\frac{\bar{V}_z}{\bar{V}}\right) \tag{10}$$

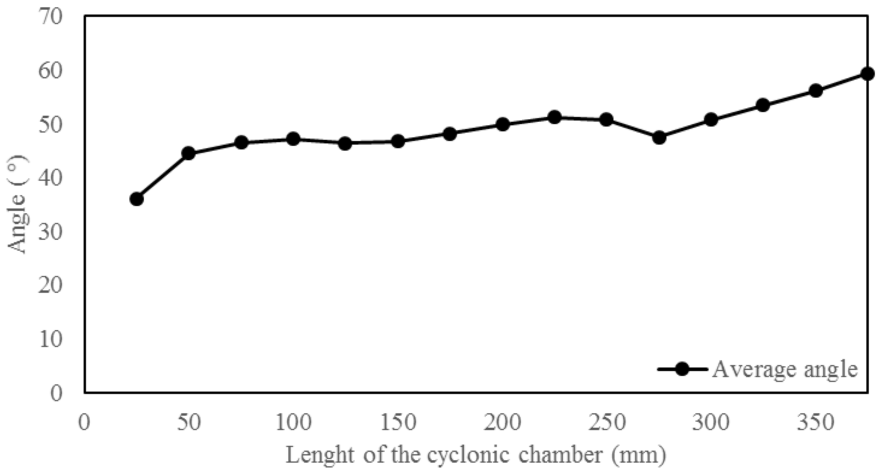

Figure 8. Average angle of the streamline along the length of the cyclonic chamber.

4. CONCLUSIONS

This paper presents numerical study of the behavior of a flow of a rising liquid film under the effect of centrifugal and gravitational fields inside the cyclonic chamber of a distributor. The division phase at the distributor outlets, the liquid film behavior, the thickness, the inclination angle of the current lines and the velocity inside the cyclone chamber are the purpose of the present study.

The division of the analysis phase of liquid and gas distributor at the four outlets are approximately equitable and the distributor is able to divide the flow equally avoiding overloads of an outlet toward other. It can also be concluded that the pattern of flow in the outlets is practically a stratified flow.

From the study concerning the liquid film behavior in the cyclone chamber it may be concluded that the average thickness increases until the cyclonic chamber height reaches 275mm, from this length on the average thickness undergoes little variation. It was observed the existence of a relation between the flow axial velocities with the behavior of the liquid film thickness average.

Finally, with the simulation, it is also noticed that the shear stress exerts greater influence than the gravitational field in the liquid film flow, and with increasing liquid film remaining inside the cyclonic chamber increases the streamline average angle.

5. ACKNOWLEDGEMENTS

The authors acknowledge the carrying out of this work to the UTFPR (Universidade Tecnológica Federal do Paraná), the NUEM (Núcleo de Escoamentos Multifásico) and PETROBRAS for the infrastructure, support and assistance for the development of numerical study of the upward liquid film flow under the effect of centrifugal and gravitational fields.

6. REFERENCES

Ansys, Inc. ANSYS-CFX® – SOLVER THEORY GUIDE, 2015.

Barnea, D., Shoham, O., Taitel, Y., 1982, “Flow Pattern Transition For Vertical Downward Two Phase Flow”, Chemical Engineering Science, Great Britain.

Morandin, M., 1999, “Modelagem De Um Filme Líquido Sob A Ação Combinada Dos Campos Centrífugo E Gravitacional De Forças: Hidrociclone,” Campinas, Brazil.

Ninahuanca, H. M.; Stel, H., 2013, “Characterization Of The Flow Dynamics In The Expansion Chamber Of A Cyclonic Separator”, 22nd International Congress of Mechanical Engineering (COBEM 2013), Ribeirão Preto, São Paulo, Brasil.

Ninahuanca, H. M.; Stel, H., 2015, “Study Of The Nozzle Diameter Influence In The Fluid Dynamics Of A Cylindrical Hydrocyclone Separator”, IV Journeys in Multiphase Flows, Campinas, São Paulo, Brasil.

Ofuchi, E., Stel, H., Franco, A., Genaro, J. and Morales, R., 2012, “Numerical Study of the Free Surface Flow in a Centrifugal Gas-Liquid Separator,” International Mechanical Engineering Congress & Exposition IMECE2012, ASME, Houston, Texas, USA.

Sant'anna, F., 2010, “Simulação Numérica do Escoamento na Câmara de Expansão do Separador Líquido-Gás VASPS,” Monograph, Universidade Tecnológica Federal do Paraná, Brasil.

Wilcox, D. C., 1998, “Turbulence Modeling For CFD”, 2ª Ed. La Canadá, CA, E.U.A.: Editor DCW Industries.

Yeoh, G. H., Tu, J., 2009, "Computational Techniques for Multi-phase Flows". Elsevier.

7. RESPONSIBILITY NOTICE

The authors are the only responsible for the printed material included in this paper.